

Optimized simultaneous planning of storage batteries and DFACTS devices

EHSAN JAFARI

Department of Electrical Engineering, Lenjan Branch, Islamic Azad University, Isfahan, IRAN

Abstract: The planning of battery energy storage system and distributed flexible transmission system (DFACTS) devices in a distribution network with the objective to reduce losses and improve the static voltage stability is the issue at hand. The storage systems' optimal location and size is determined by considering installation costs to reduce power losses. To minimize power losses in the network, the energy storage and DFACTS devices are coordinated for the first time, where the investment costs of these devices are of concern. In the available studies, only the issue of economic approach is of concern. In this study, in addition to the economic approach, the problem of improving the static voltage stability is of concern, where the multi-objective problem will be evaluated as well. The optimum utilization of the storage, by applying the fuzzy controller is presented in this study to reduce power losses in the distribution network. The problem is evaluated at different load levels and in the presence of distributed generation resources in the network. The two-objective optimization is implemented by applying the multi-objective particle swarm and non-dominated sorted genetic algorithm, and the results are compared.

Keywords: power losses, storage batteries, voltage stability, multi-objective problem.

Received: May 15, 2021. Revised: February 17, 2022. Accepted: March 15, 2022. Published: April 5, 2022.

Nomenclature

$\bar{U}_k^{*(j-1)}$	Bus voltage in the previous iteration	S	Surface being traversed by turbine blades (m ²)
\bar{Z}_k	Series impedance of the k-th branch	ρ	Density of air in terms of kg/m ³
\bar{E}_0	Base node voltage, or slack bus	R	Rotor radius (m)
$d\bar{U}$	Voltages drop vector in each $k - th$ branch	V_{wind}	Wind speed (m/s)
η_{sd}	Self-discharge coefficient and	λ	Tip speed ratio
η_c / η_d	Charge /Discharge efficiency	V_i	Bus voltage
$P_{st,c} / P_{st,d}$	Charge /Discharge modes of BESS	V_M	DSTATCOM voltage
SOC	BESS capacity	X_L	Line reactance
T_c / T_d	Minimum charge/ discharge time	δ	Voltages V_M and V_i angle difference
I_{ph}	Photo-current subject to the intensity of the radiation and temperature	$cost_{BESS,i} / cost_{DSTAT,i}$	cost of installing each BESS / DSTATCOM unit at \$/kwh and \$/kVAr
I_d	Polarization of the PN bonding current	$ccap_{BESS,i} / cap_{DSTAT,i}$	Capacity of BESS / DSTATCOM
I_{Rsh}	Resistance R_{sh} current	k_i	Cost of energy losses (kwh)
$P_{loss}(t_i)$	Total network losses at the $t_i - th$ time interval	NoB	Count of network buses
N/n	Count of time interval studied /total count of nodes	w_1 / w_2	Weight of each of the objective functions are equal 0.5.
V_i / V_{ref}	Bus voltage magnitude/ reference voltage of $i - th$ bus		

1. Introduction

Motivation and incitement: Reduction of network losses is one of the main challenges for distribution networks beneficiaries. The batteries are able to reduce network losses with proper allocation and energy management in the network, and increase the penetration of renewable distributed generation (DG) units

and batteries participation in voltage regulation through their inverters [1-4].

Literature review: Although FACTS devices are to improve power quality issues in power transmission systems, a similar device can be applied to improve power distribution systems. Distribution static compensator (DSTATCOM) is one of these devices, usually applied in distribution systems to improve power

quality, voltage regulation, voltage balance, harmonic reduction, voltage flicker compensation, stability improvement, load balance etc. [5,6].

The DG, based on renewable resources like wind, photovoltaic, fuel cells, etc. have been and are of particular importance for reasons like greenhouse gas reduction, energy losses reduction, voltage profile improvement and reliability. Some of these resources are random in nature and will be variable and non-deterministic [7]. The load demand is variable, thus, a reason to change the compensator capacity needs to be changed with the appropriate response subject to different load conditions, like the DSTATCOM [6].

There exist many studies run on DSTATCOM. The problem of locating this compensator is assessed by [8], according to the network restructuring view with the objective to reduce power losses and improve voltage profiles by particle swarm optimization (PSO), where, the loads of 69 and 83-bus IEEE test systems are considered constant in terms of their base values.

The immune optimization algorithm is applied to DSTATCOM in the presence of DG, with the objective to reduce active losses and improve voltage and current profiles of the network by modifying the network load as a three-level load pattern, regardless of load growth, is modeled in [9].

The simultaneous placement of DSTATCOM and DG, the multi objective optimization method, modified PSO with the objective to reduce the cost of losses and improve the voltage through constant load profile in the 33 and 69-bus IEEE test systems are assessed in [10]. The exhaustive search method algorithm and 30-bus radial distribution system are optimized in [11].

The simultaneous placement of DSTATCOM and DG to improve voltage profiles and reduce losses by considering cost using bacterial search optimization algorithm in 33 and 115-bus IEEE systems are assessed in [12], although the test systems loads are constant and equal to their basic load. The cuckoo search algorithm with voltage stability index and losses sensitivity factor is applied in 12, 34 and 69-bus IEEE sample systems by [13]. The Losses Reduction and Voltage Profile Improvement, together with the Direct Load Flow method, are applied to optimally accommodate DG and DSTATCOM in a 33-bus test system over a one-year period in [14].

The bat optimization algorithm for DSTATCOM considering load variations is applied in [15], where, the load variations are modeled as step size with three-level load variations from light to peak load.

Both the photovoltaic array allocation problem and DSTATCOM is assessed in a simultaneously with the objective to improve voltage profile and reduce power losses in [16, 17]. fuzzy- ant colony optimization algorithm without considering load changes studied in [16]. where, the photovoltaic array is modeled

regardless of uncertainty as a DG. The problem of network restructuring with the objective to reduce losses and consider the losses cost through the GA-fuzzy method in 33 and 69-bus IEEE test systems in [17].

Contribution and paper organization: As to the title of this article the optimal placement and size of BESS is determined by considering installation costs to power losses reduction. To reduce power losses in the network, the coordinated BESS and DFACTS devices are proposed, where, the investment cost of these devices are of concern for the first time. On the other hand, in previous studies, storage development programming problem has been considered only with the economic approach. In this study, next to the economic approach, the problem of improving the static voltage stability is of concern and is evaluated in two objectives. The optimum utilization of the storage through the fuzzy controller is another suggestion of this study which is proposed to reducing more power losses on the distribution network. It is noted that the problem is evaluated at different loading levels and in the presence of distributed generation sources in the network. Also the optimization, due to the two objective of the problem, is compared using multi-objective GA and PSO and related results.

This article is organized as follows: the system modeling is presented in Sec.2; the problem is formulated in Sec.3.

the optimal size and location of the storage system are determined in Sec.4. The networks are diagram in Sec.5; the, simulations and results are presented in Sec. 6 and the article is concluded in last Sec.

2. System modeling

The main step in distribution network studies is components modeling and run the load flow calculation therein.

2-1 Network modeling and optimal load distribution

Due to the radius of the subject distribution networks, the backward - forward sweep method (BFSM) is applied. For this load flow, the impedance of all lines, the active and reactive load of buses must be specified. The positive sign of the power indicates the load availability and the negative sign indicates the generator.

2-1-1 Matrix model of network

This topology is quite arbitrary, subject to the terms set in advance. The following constraints must be met:

- The radial structure of the network is indicative of the number of network nodes must be equal to the number of branches
- The numbering begins from the location of the sub-transmission substation.

- All values will be expressed in terms of physical dimension.

2-1-2 Network topology matrix

To express this matrix, two incidence matrix nodes with branches (A) and path matrix (P) are applied. The A- reduced matrix is defined as, $A \in N^{n,n}$ (node \times branch), a square matrix due to the radial properties of the distribution network. The node at the beginning of the branch is known as -1 and node at the end with +1. The path matrix $P \in N^{n,n}$ (node \times branch) is defined as: if the k -th branch belongs to the path that connects the j -th node to the base node, then value one is assigned, otherwise zero. According to the if-then above, it can be said that equation $-[A][P]=[I]$ is established.

2-1-3 Calculating the voltage and current

After defining the network matrix, the network voltage and current are determined by the iteration in the BFSM algorithm, where, the current drawn by each bus in the j -th iteration the load distribution is calculated through. Eq. (1):

$$\bar{I}_{nk}^{(j)} = \frac{\bar{S}_k^*}{3\bar{U}_k^{*(j-1)}} \quad (1)$$

By computing node current, branch current is computed as E.q (2):

$$[A]\{I_b^{(j)}\} = \{I_n^{(j)}\} \quad (2)$$

After calculating the lines' current through Eqs.(1 and 2), the voltage drop over each line is calculated through Eq.(3):

$$d\bar{U}_k^{(j)} = \bar{Z}_k \bar{I}_{bk}^{(j)} \quad (3)$$

where, the voltage of each bus in each iteration is calculated through Eq.(4):

$$\{\bar{U}^{(j)}\} = \bar{E}_0 - [P]\{d\bar{U}^{(j)}\} \quad (4)$$

The load flow iteration process continues until the following convergence condition is met:

$$\left| \frac{\{\bar{U}^{(j)}\} - \{\bar{U}^{(j-1)}\}}{\{\bar{U}^{(j-1)}\}} \right| \leq \varepsilon \quad (5)$$

The Backward/Forward Sweep Method (BFSM) load flow iteration process terminates when the voltage difference between two consecutive iteration is less than the small constant ε volume.

2-2 Modeling the BESS

To model the storage system, BESS is considered as a passive element, therefore, power is injected into the BESS with a positive sign and the power generated, thereof is shown with a negative

sign. The state of charge (SoC) at time $t + 1$ is expressed through Eq. (6):

$$SOC(t_i + 1) = \eta_{sd} SOC(t_i) + \left(\eta_c P_{st,c}(t_i) - \frac{P_{st,d}(t_i)}{\eta_d} \right) \Delta t \quad (6)$$

The injection and absorbed power of the BESS should be applied within the range expressed through Eqs. (7-9):

$$0 \leq P_{st,c} \leq \delta_c \frac{SOC_{max}}{T_c} \quad (7)$$

$$0 \leq P_{st,d} \leq \delta_d \frac{SOC_{max}}{T_d} \quad (8)$$

$$0 \leq \delta_c + \delta_d \leq 1 \quad (9)$$

Eq.(9) is a logical relation where δ_c and δ_d are binary variables that cause simultaneous charge and discharge not happen at the same time. The technical specifications and parameters required in modeling BESS are presented in [18].

The BESS is connected to the AC grid by the inverter, allowing it to generate active and reactive power on the AC side by the means of the inverter's capability curve. The performance of the inverter in terms of active and reactive power is shown in this diagram. Therefore, the active and reactive power exchanged by the inverter is subject to the bus voltage and current of the BESS.

$$\bar{S}_{st} = 3\bar{I}_{st}^* = P_{st} + jQ_{st} = (P_{st,c} - P_{st,d}) + jQ_{st} \quad (10)$$

where, the reactive power exchanged by the inverter can be either positive or negative. Consequently, in each iteration of load flow, the relation between the active and reactive power is exchanged and the active and reactive component of BESS current connected to K -th bus is calculated through Eqs.(11 and 12):

$$\Re[\bar{U}_k^{(j-1)}] \Re[\bar{I}_{st}^{(j)}] + \Im[\bar{U}_k^{(j-1)}] \Im[\bar{I}_{st}^{(j)}] = \frac{P_{st,c}^j - P_{st,d}^j}{3} \quad (11)$$

$$\Im[\bar{U}_k^{(j-1)}] \Re[\bar{I}_{st}^{(j)}] - \Re[\bar{U}_k^{(j-1)}] \Im[\bar{I}_{st}^{(j)}] = \frac{Q_{st}^{(j)}}{3} \quad (12)$$

2-2-1 BESS inverter capability curve

The BESS are connected to the radial distribution network by the inverter and can be controlled by the grid operator to work at every four quadrants of the capability curve [19]. The objective is to exchange the reactive power between the BESS inverter and the network in order to reactive compensation and reduce power losses. The ability of the inverter to generate the active and reactive power within its performance range is represented in Fig. 1.

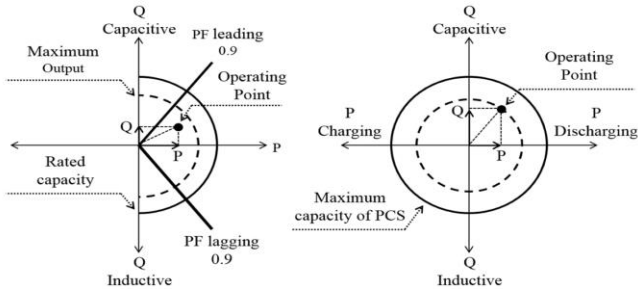


Fig. 1: The BESS Inverter capacity curve

According to this curve, the active and reactive power exchanged by BESS is limited, Eqs. (13 and 14):

$$P_{st,c}^2 + Q_{st}^2 \leq S_{max}^2 \quad (13)$$

$$P_{st,d}^2 + Q_{st}^2 \leq S_{max}^2 \quad (14)$$

where, the reactive power generation is limited and expressed as:

$$Q_{st,min} \leq Q_{st} \leq Q_{st,max} \quad (15)$$

To simplify the problem, the maximum complex power (S_{max}) of the inverter is considered to the maximum power of BESS. If BESS power coefficient is limited due to its technical specifications, then the capability curve of the inverter is constrained by another linear equation, defined in Fig. 1 in the red zone, and expressed in details through Eqs.(16-20):

$$Q_{st,c} - P_{st,c} \tan \varphi_{lim} \leq 0 \quad (16)$$

$$Q_{st,c} + P_{st,c} \tan \varphi_{lim} \geq 0 \quad (17)$$

$$Q_{st,d} - P_{st,d} \tan \varphi_{lim} \leq 0 \quad (18)$$

$$Q_{st,d} + P_{st,d} \tan \varphi_{lim} \geq 0 \quad (19)$$

$$Q_{st} = Q_{st,d} + Q_{st,c} \quad (20)$$

These equations assure that the reactive power generated by BESS inverter meets the power factor limit at both the charge and discharge states.

2-3 DSTATCOM modeling in distribution network

DSTATCOM is one of the FACTS devices usually consisting of a coupling transformer, a power electronic voltage converter, and a capacitor. The active and reactive power of DSTATCOM are expressed through Eqs. (21 and 22):

$$P_{DSTATCOM} = (V_i V_M / X_L) \sin \delta \quad (21)$$

$$Q_{DSTATCOM} = (V_i^2 / X_L) - (V_i V_M / X_L) \cos \delta \quad (22)$$

2-4 Model of renewable energy sources

The two photovoltaic and wind turbine systems are applied as DG units in the network. In order to model these units 2-4-1 and 2-4-2 sections are presented [3].

2-4-1 Photovoltaic system

There exist, different mathematical models proposed in describing the nonlinear behavior of photovoltaic systems due to their semiconductor joints. The model shown in Fig. 2 is applied for photovoltaic system:

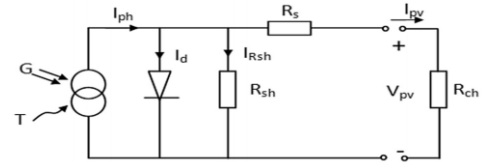


Fig. 2: Equivalent circuit of solar cells

The photovoltaic cells current (I_{pv}), subject to standard conditions is obtained through Eq.(23):

$$I_{pv} = I_{ph} - I_d - I_{Rsh} \quad (23)$$

The flow of solar cells is expressed through Eq. (24):

$$I_{pv} = I_{sc} \left\{ 1 - K_1 \left[\exp(K_2 \cdot V_{pv}^m) - 1 \right] \right\} \quad (24)$$

where, K_1 , K_2 and m are the constants obtained through Eqs. (25-29):

$$K_1 = 0.01175 \quad (25)$$

$$K_2 = \frac{K_4}{V_{oc}^m} \quad (26)$$

$$K_3 = \ln \left[\frac{I_{sc} (1 + K_1) - I_{mpp}}{K_1 \cdot I_{sc}} \right] \quad (27)$$

$$K_4 = \ln \left[\frac{1 + K_1}{K_1} \right] \quad (28)$$

$$m = \frac{\ln \left[\frac{K_3}{K_4} \right]}{\ln \left[\frac{V_{mpp}}{V_{oc}} \right]} \quad (29)$$

The Eq.(24) is applied only in standard test conditions ($G=1000$ W/m² and $T = 25$ °C). Whenever the solar radiation and air temperature are not of standard volumes of the test, the model parameters would change according to Eqs. (30-32):

$$\Delta T_c = T_c - T_{STC} \quad (30)$$

$$\Delta I_{pv} = \alpha_{sc} \left(\frac{G}{G_{stc}} \right) \Delta T_c + \left(\frac{G}{G_{stc}} - 1 \right) I_{sc, stc} \quad (31)$$

$$\Delta V_{pv} = -\beta_{oc} \Delta T_c - R_s \Delta I_{pv} \quad (32)$$

By applying the mentioned model in the software, the power-voltage diagram P_{pv} (V_{pv}) and the current-voltage diagram I_{pv} (V_{pv}) of the photovoltaic panel are under the three different conditions of radiation and air temperature are studied in [20]. Due to the nonlinear nature of current and power characteristic, Therefore, to obtain maximum power from this system, must force the system to work at a maximum power point. Parameters of the SUNTECH solar panel applied in this study are presented in Appendix.

2-4-2 Wind turbine model

The subject wind generator is composed of a blade that absorbs the kinetic energy of the wind and a coupled synchronous generator to convert the kinetic energy into electrical power through a rectifier to power the DC bus.

The output power and torque of the wind turbine are calculated through Eqs. (33 and 34):

$$P_{wind} = \frac{1}{2} C_p(\lambda) \cdot \rho \cdot S \cdot V_{wind}^3 \quad (33)$$

$$T_{wind} = T_{mec} = \frac{1}{2} \frac{C_p(\lambda) \cdot \rho \cdot R \cdot S \cdot V_{wind}^2}{\lambda} \quad (34)$$

3. Problem formulation

3.1. Definition of objective functions

The objective functions considered in this problem consist of two economic and technical objective functions: the first is the cost of the existing storage system and DFACTS devices, and the second consists of energy losses and static voltage stability in the network.

3-1-1 Investment cost objective function

This objective function is of: investment cost of storage systems and DFACTS devices, each calculated through Eqs.(35-37):

$$C_1 = \sum_i (\text{cost}_{BESS,i} \times \text{cap}_{BESS,i}) \quad (35)$$

$$C_2 = \sum_i (\text{cost}_{DSTAT,i} \times \text{cap}_{DSTAT,i}) \quad (36)$$

$$OF_1 = C_1 + C_2 \quad (37)$$

3-1-2- Technical objective function

Reducing losses and improving the voltage profile are the main objectives in distribution networks, consisting of DG resources, BESS and DFACTS devices, where, location and capacity of the equipment are determined to bring the network voltage magnitude be closer to the reference volume. Eq. (38) describes the objective function covering the goal.

$$P_{LOSS} = \sum_{i=1}^N (P_{loss}(t_i) \times k_i) \quad (38)$$

$$P_{loss} = \sum_{i=1}^N \sum_{k=1}^n 3R_k \left| \bar{I}_{bk}(t_i) \right|^2 \quad (39)$$

$$JV = \sqrt{\sum_{i=1}^{NoB} |V_i - V_{ref}|} \quad (40)$$

$$OF_2 = w_1 \cdot P_{LOSS} + w_2 \cdot JV \quad (41)$$

By minimizing this objective function, it is possible to bring the voltage of different phases of the network as close as possible to the reference volumes.

3-2 Optimization process

The non-dominated sorting genetic algorithm (NSGAI) is applied to determine the optimal capacity of BESS and DFACT devices. The simulation of the multi objective particle swarm optimization algorithm (MOPSO) is run and compared with the results of the NSGAI. The multi-objective optimization problems usually have different solutions, that is, they are none dominant.

To obtain the answers, two types of methods are proposed:

a-The methods that transforms the multi-objective problem by combining the objective functions into single-objective problem, is the most applicable method in this category of weighted sum methods. In this method, different objective functions are combined through appropriate weighting coefficients in a single objective function to be assessed by single-objective optimization methods. The major drawback of these methods is in obtaining appropriate coefficients which requires extensive knowledge on the optimization problem. Determining the final solution depends on the selection of appropriate weighting coefficients and it is usually possible to rearrange the coefficients by changing the subject sample under study.

b-The methods that obtain the answers to the problem by applying the dominancy concept with respect to all the goal-problem functions, are usually the most effective. Solving a multi-objective optimization problem leads to formation of an optimal solution set. With respect to all objective functions, there is no response to the other, this set of optimal solutions is named the Pareto optimal or effective solutions. Most multi objective optimization algorithms apply the dominance concept to find the Pareto optimal. The concept of dominance with respect to the minimization problem in its Mathematical sense is expressed as:

Let say the set of answers c be dominated by the set of answers X_2 , if the following two conditions are met at the same time:

1. The answer X_1 for all objective functions is not worse than X_2 .

$$\forall i \in [1, 2, \dots, m] : f_i(X_1) \leq f_i(X_2) \quad (42)$$

2. The answer X_1 of X_2 is better at least by one objective function.

$$\exists i \in [1, 2, \dots, m] : f_i(X_1) < f_i(X_2) \quad (43)$$

All non-dominant solutions constitute a region, where, a Pareto front is called. In this region, none of the answers are dominant, and the final optimal solution is determined by decision maker.

4. Determining the optimal size and location of the storage system

The proposed optimization procedure in section 2-3 with the use of fuzzy controllers can be used to manage the recharge of the BESS and reduce network losses. The BESS can be connected to each network bus of any size, but it is necessary to determine the optimal size and location for installation to maximize losses reduction and minimize investment costs.

4-1- Determining the optimal location of BESS installation by sensitivity analysis

To install storage systems, the buses, where, these devices have little effect on network losses should be of concern. To decrease losses and save cost, the installation of these systems must be implemented in buses, with the highest sensitivity to losses. These buses can be identified by sensitivity analysis to power losses.

To do so, both the load profile and constants are added to the k -th bus of the network and the power losses of $P_{\text{losses},k}$ is calculated during the day for the network, before and after adding the load. Following this, an index is defined according to the following equation to measure the k -th bus sensitivity to power losses:

$$\sigma_{\text{LOSS},k} = \frac{P_{\text{LOSS},k} - P_{\text{LOSS}}^*}{P_{\text{LOSS}}^*} \times 100 = \frac{\Delta P_{\text{LOSS},k}}{P_{\text{LOSS}}^*} \times 100 \quad (44)$$

This process is repeated for each bus and the results are presented as a sorted list of most sensitive buses which is applied in installing the storage systems.

4-2-Energy management in BESS through fuzzy controller

In this study, it is used to control power flow from the fuzzy control system. This system uses fuzzy logic to connect its input and output. The general structure of a fuzzy system consists of four main sections: fuzzy, control structure and decision maker, non-fuzzy and fuzzy system rules. Fuzzy system rules consist of rules for different input and output connections. The output of the

fuzzy system is a fuzzy variable that must be converted into a numeric volume through the non-fuzzy system. In this article, the mass center method is applied for Non-fuzzification. The existence of DG and storage units in the network, necessitates a control system to control the energy flow between the generators, loads, storages and upstream network. The objective of this proposed fuzzy control system is to manage the energy flow in the network by establishing a logical power balance between the production and consumption, time control and battery charge and discharge, time control and power exchange rate with the upstream network. For this purpose, two fuzzy control inputs are considered. The input, output and fuzzy rules of this proposed fuzzy control system are tabulated in Table 1.

The first input is the network load profile (LP) with three membership functions (linguistic variables) of *low*, *med* and *high*, respectively. Another input is the per-unit battery SoC based on battery capacity in terms of three membership functions *low*, *med* and *high*. The output of the fuzzy system is the control signal for controlling the battery the charge and discharge. This output is named STATE, with four membership functions of BDE, SDE, SCH and BCH respectively, fuzzy system output is a control signal as to control the charge and discharge battery, that is the *high power discharge*, *low power discharge*, *low power charging* and *high power charging*, respectively. The membership functions of this proposed fuzzy control are shown Fig. (3).

5- Radial Distribution Network

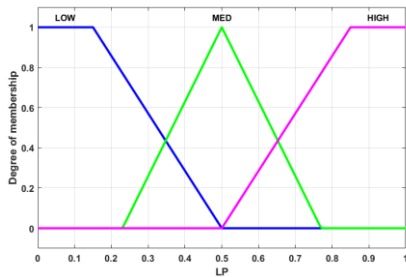
To implement the algorithms and this proposed method in the previous section, we need a network. In this study, a CIGRE radial and medium voltage(MV) distribution network and a 17-bus radial distribution network are applied.

5-1 Case study A

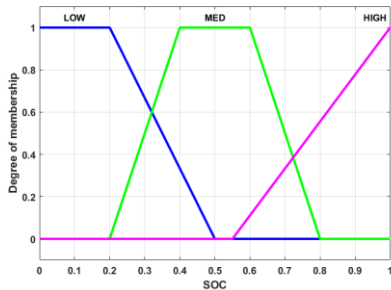
It is a 14-bus network connected to the high voltage(HV) sub-transmission system through two HV/MV transformers, Fig. (4).

Table 1: Fuzzy rules of this proposed fuzzy control system

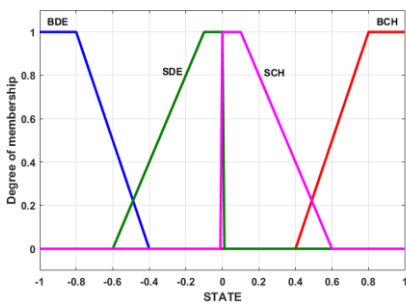
LP	SOC	STATE
LOW	LOW	BCH
	MED	BCH
	HIGH	SCH
MED	LOW	SCH
	MED	SDE
	HIGH	SDE
HIGH	LOW	SCH
	MED	BDE
	HIGH	BDE



(a)



(b)



(c)

Fig. 3: Membership functions of this proposed fuzzy control system(a): Load profile, (b): State of charge, (c): output of the fuzzy system

To model this network, each one of the transformers is modeled using a line with the secondary equivalent impedance of transformers. In this network, the first three S_1 , S_2 and S_3 switches are embedded to change the network layout. In this article, it is assumed that all three switches are ON. The renewable energy sources are considered in assessing these networks. For this purpose, it is assumed that bus 10 of this network is a distributed solar generation unit with a capacity of 1000 kw and bus 11 is a wind unit with a capacity of 800 kw.

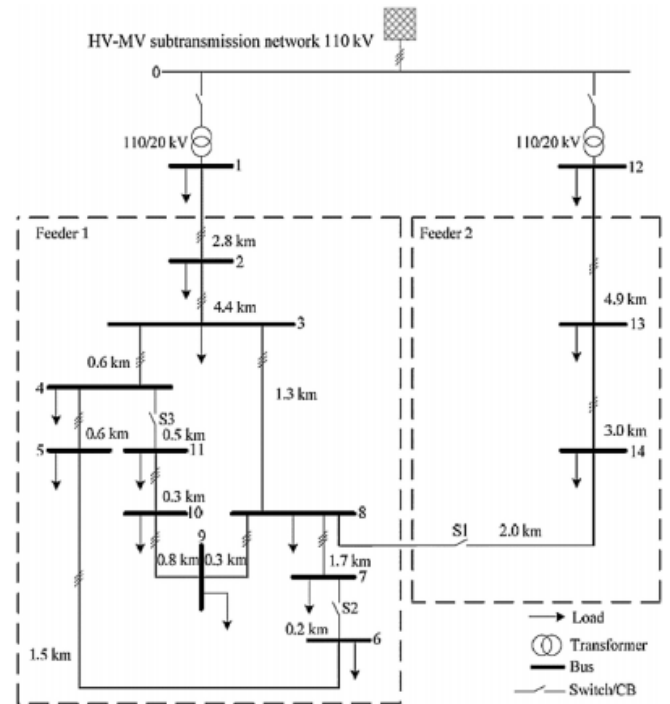


Fig. 4: CIGRE MV testing network

The transformer information of this network, the data on its lines and the load information are tabulated in Appendix. The active and reactive load of the test network A is shown in Figs. (5 and 6).

5-2 Case study B

A 17-bus network is connected to the high voltage (HV) sub-transmission system through a single HV/MV transformer, Fig.(7). The information of the network and its loading information are in Appendix. The load profile of the network during a day is shown in Fig. (8).

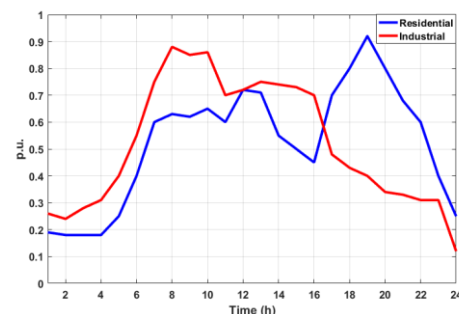


Fig. 5: Active load profile of the test network A during the day

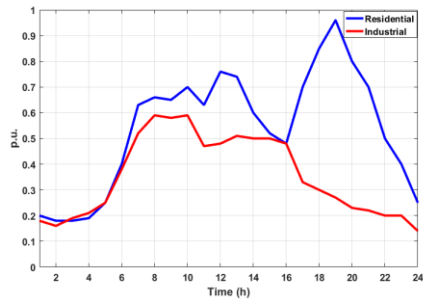


Fig. 6: Reactive load profile of the test network A during the day

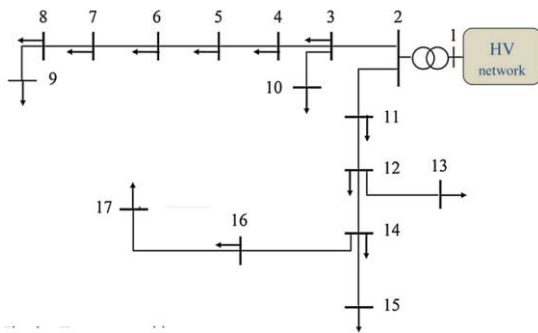


Fig. 7: MV distribution network case study B

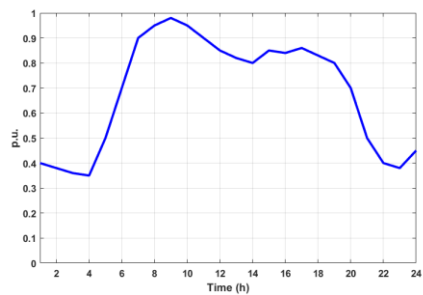


Fig. 8: load profile of the B test network

As observed in Table 2, the sensitivity coefficients of buses 3 to 11 are higher than other network buses, thus, their candidacy in being selected for BESS installation. It is assumed that buses 10 and 11 are of solar units, respectively, with a nominal capacity of one megawatt and wind unit with a nominal capacity of 800 KW. The power generation of these units is calculated in one-day period based on the radiation, temperature and wind speed information, Fig. (9).

The optimization of the NSGAII for a sample of simulations at 0.75 storage power factor is shown in Fig. (10), where, the first objective function is the economic and the second is the technical objective function of the problem. Here, none of the Pareto optimal points are dominant, and determining the optimal point is responsibility of the decision maker. Here, the point is chosen where both the objective functions are minimal.

Table 2: Sensitivity of the A test network to power losses

Bus	$\sigma_{loss,k}$ (%)
2	8.8
3	21.9
4	22.6
5	23.1
6	23.9
7	25.5
8	24.4
9	24.9
10	25.6
11	25.7

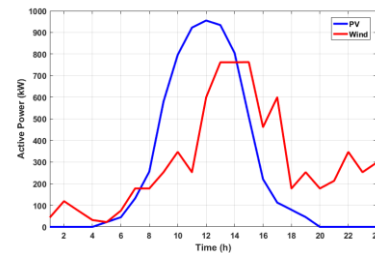


Fig 9: Power generation of renewable DG units of test network A

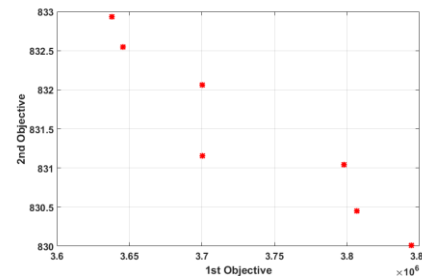


Fig 10: Pareto points derived from NSGAII

6. Simulations and results

Here, only buses with greater sensitivity to power losses are candidates for BESS installation. The simulations are run in an Intel Core i3 processor with 1.8 GHz and 4GB of RAM by using the MATLAB interface for GUROBI optimizer.

6-1 The test network A results

To determine the location of the storage system in this network, the sensitivity analysis is run, where, the constant load of 500 KW with unit power factor is added to each bus and the sensitivity index is calculated. The most sensitive network buses' loads in terms of losses are tabulated in Table 2. The more sensitivity factor a bus, the more prone to be installed in storage.

The simulation results of the optimal storage capacity for different power factors are shown in Fig. (11). In general, when the power factor is limited (for example $\cos \varphi_{lim} = 0.75$), the storage capacity increases; because of the inverter capability curve, the battery can generate more reactive power if it has more active power. On the contrary, if there is no power factor limitation ($\cos \varphi_{lim} = 0$), the battery will have low capacity, because reactive power in the inverter can be generated if no active power is available. The changes in SoC for the power factor of unit and zero during the day are shown in Fig. (12 a and b) respectively. To maintain battery durability, the charge level must be kept at 10 % of the capacity at the least throughout the day.

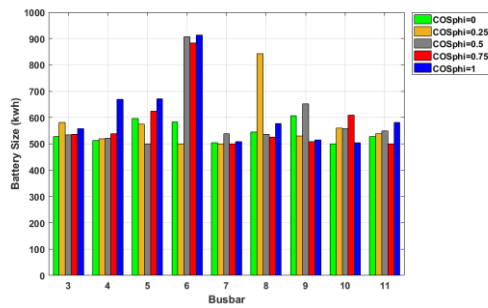
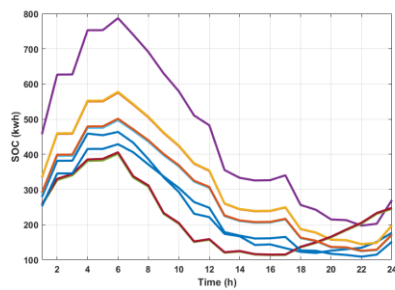
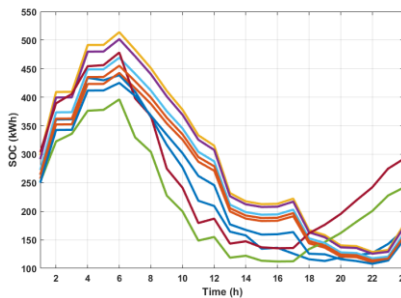


Fig 11: Optimal storage capacity at different power factors in the test network A



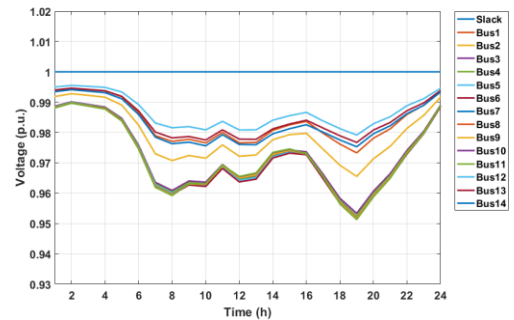
(a)



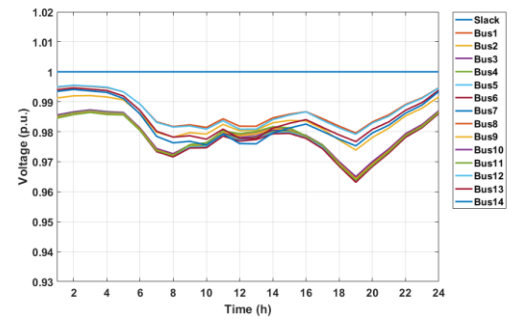
(b)

Fig 12: Comparison of the SoC of batteries connected to the sensitive buses of a network in two cases a: $\cos \varphi_{lim} = 1$ and b: $\cos \varphi_{lim} = 0$

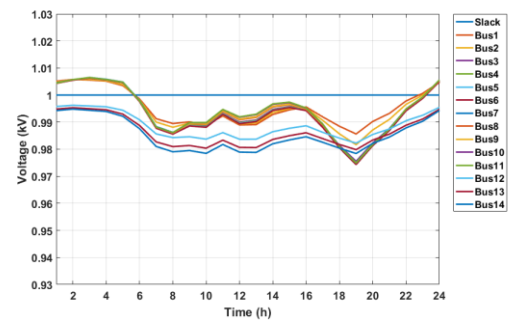
One of the objective functions in the available studies is the network static voltage stability, which is to improve the network buses' voltage in the three modes without BESS, with zero and one power factor structural reserve, Fig. (13). According to this diagram, the network buses' voltage in the non-storage mode is greater than its reference volume and its profile is not planar. Applying the battery power factor (without reactive power production) reduces network voltage drop, while, applying zero power factor batteries reduces the voltage drop and generates a flatter voltage profile.



(a)



(b)



(c)

Fig 13: Buses voltage profiles of the test network. A: a) without storage, b) with storage $\cos \varphi_{lim} = 1$ and DFACTS and c) with storage $\cos \varphi_{lim} = 0$ and DFACTS

One of the important effects of BESS in the network is its flattening the current profile of the network lines, that is, reducing the system losses. The current amplitude of the lines 6 and 9 of the network during the day, with and without BESS, and with D-STATCOM and at different inverter power factors are shown in Figs. (14 and 15), where, placing BESS in sensitive points of the network significantly flattens the current profiles and reduces losses. This effect is observed both in unit power factor (without reactive power generation) and in states where reactive power is generated.

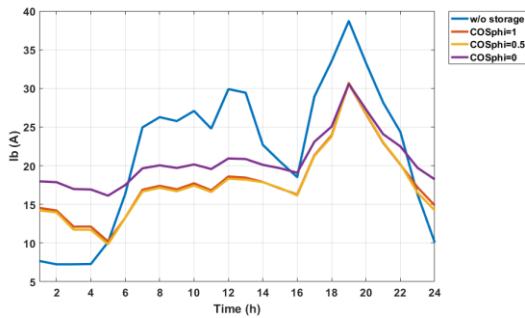


Fig 14: Branch 6 current in test network A at different power factor

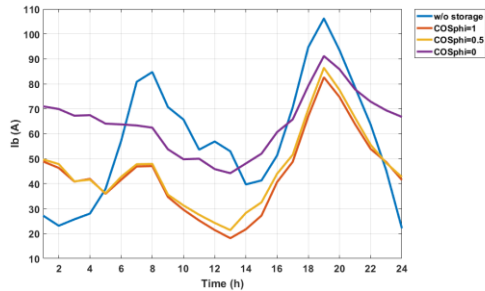


Fig 15: Branch 12 current in test network A at different power coefficient

The reactive power generated by the inverter is highly depends on the battery connection load topology. Considering that bus 6 is only lighting load, Fig. (16), the reactive power of DSTATCOM through of the normalized lighting load profile. As observed in Fig. (17), the reactive power generation of the STATCOM in bus 9 is depend on the industrial load profile of bus 9. The reactive power generation of the STATCOM in bus 3, according to load

profile, a combination of lighting and industrial loads, is shown in Fig. (18).

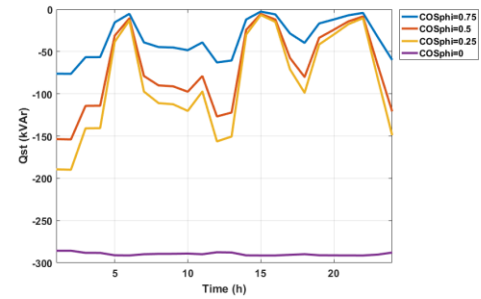


Fig 16: Variation of the reactive power generation of the DSTATCOM in bus 6 on the test network A

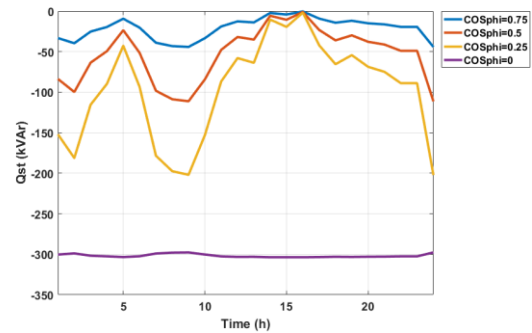


Fig 17: Variation of the reactive power generation of the DSTATCOM in bus 9 on the test network A

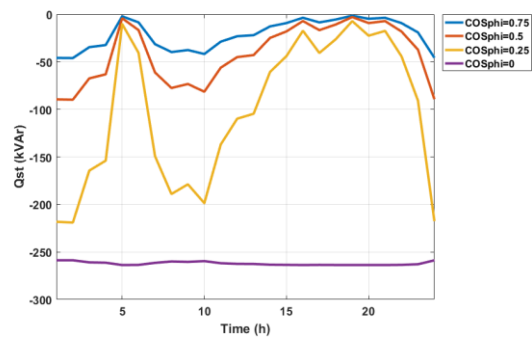


Fig 18: Variation of the reactive power generation of the DSTATCOM in bus 3 on the test network A

All simulations are run by applying the NSGAI multi objective algorithm, while, to compare the simulations the MOPSO algorithm is applied and the results of the two algorithms are compared, Table 3, where, as observed, the results are closes.

Table 3: Comparison of simulation results obtained through the MOPSO and NSGAI algorithms for the test network A

$\cos \varphi_{lim} = 1$	$\cos \varphi_{lim} = 0.75$	$\cos \varphi_{lim} = 0$	BESS	Algorithm	
9	4	13	-	NSGAI	D-STATCOM Location
9	4	13	-	MOPSO	
1281	1040	860	-	NSGAI	D-STATCOM Capacity (kVAr)
1280	1040	880	-	MOPSO	
811	815	1304	2438	NSGAI	Losses (kW)
812	815	1310	2438	MOPSO	

6.2. Results of the test network B

The results of the sensitivity analysis of this network are tabulated in Table 4, where, buses 16 and 17 are more sensitive than other buses, so this bus is chosen for BESS installation. It is assumed that the buses 14 and 15 will have photovoltaic and wind power of 1000 and 800 KW, respectively. The size and location of D-STATCOM are obtained during the optimization process.

The simulation through this proposed methods, and applying a NSGAI, the BESS capacity in different powers factor is shown in Fig. (19). As observed test network A, when the power factor is finite ($\cos \varphi_{lim} = 0.75$), the battery capacity is expected to increase. Because of the inverter capacity curve, the BESS can generate more reactive power if it has more active power. On the contrary, where there is no power factor constraint ($\cos \varphi_{lim} = 0$), the BESS will have lower capacities because the reactive power in the inverter can be generated if there is no active power. In this particular network structure, where the BESS location is restricted to two bus, the BESS capacity of bus 16 is reduced by limiting the power factor to 0.75, while, in bus 17 the opposite holds true. At zero power factor of BESS, 16 bus capacity increases and reduced to 17 bus.

Table 4: The sensitivity of the test network B buses to power losses

Bus	$\sigma_{loss,k}$ (%)
6	7.5
7	7.8
8	8.9
9	11.2
12	9.6
13	10.7
14	14.6
15	14.7
16	17.3
17	17.9

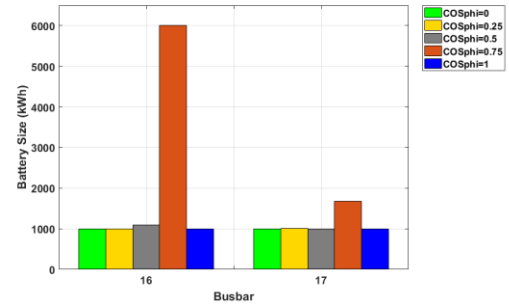
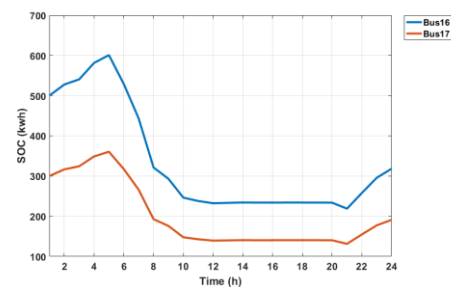
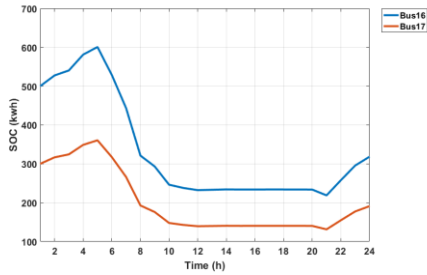


Fig 19: Optimal BESS capacity of different power factors in the test network B

The SoCs of the batteries of this network are shown in Fig. (20 a and b), where, as observed the SoC management is influenced by the load profile. Here, too, to maintain the health of the batteries, the minimum charging level is considered to be 10% of the battery capacity and is not allowed throughout the day. In general, the minimum SoC at the peak load and its maximum occurs at least load of the network. In fact, the load shift with BESS takes place at the light load and release it at the peak load. The line current of the branches 12 and 14 with and without storage and D-STATCOM and different inverter capacitors are shown in Figs. (21 and 22), where, as observed, placing BESS at sensitive points in the network flattens the line current profile and decrease losses. This effect is observed both in unit power factor (without reactive power generation) and when the reactive power is generated.



(a)



(b)

Fig 20: Comparison of the SoC connected to sensitive buses of B networks in two cases a: $\cos \varphi_{lim} = 1$ and b: $\cos \varphi_{lim} = 0$

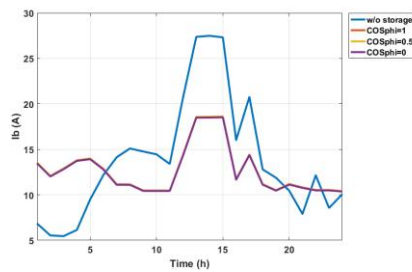


Fig 21: Branch 14 current of the test network B at different power factors

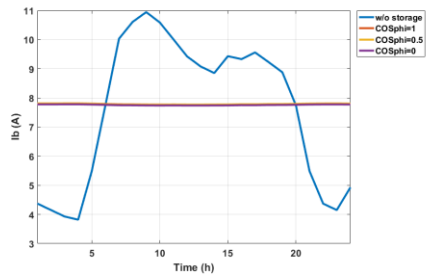
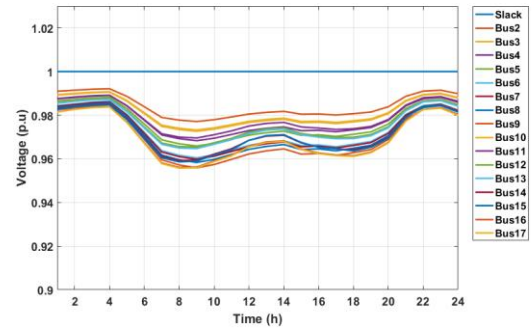
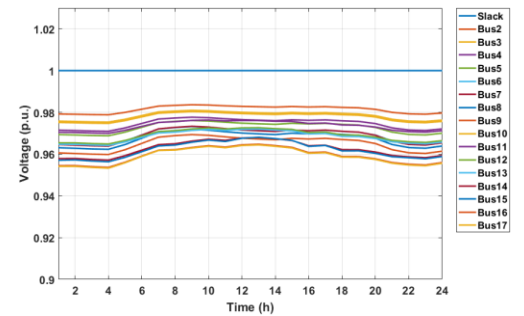


Fig 22: Branch 12 current of the test network B at different power factors

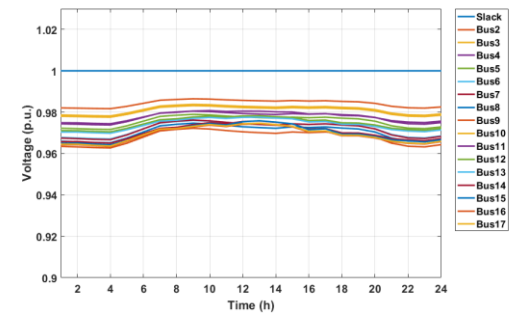
One of the objective functions considered in such studies is the static voltage stability of the network. In this article, the bus voltage is illustrated in three states of without BESS and with BESS in zero and unity power factor, Fig.23, where, the voltage of the network buses in non-storage mode has a greater distance than its reference volume and its profile is not planar. Applying BESS with a power factor of 1 (without reactive power generation) reduces the network voltage drop, while, applying BESS with a power factor of zero will reduce the voltage drop and form a flatter voltage profile.



(a)



(b)



(c)

Fig 23: Voltage profile of the test network A buses: a) without BESS, b) and c) with BESS and DFACTS in $\cos \varphi_{lim} = 1$

$\cos \varphi_{lim} = 0$ respectively

One of the most important applications of BESS inverter is the reactive compensation. Because the reactive power generated by the BESS can supply the reactive load, consequently, the reactive power of the BESS inverter, behavior is similar to the load profile. The BESS reactive power changes in bus 16, is shown in Fig. (24), where, the reactive power variations of this BESS are behavior similar to load profile of Fig. (6). To compare the simulations' results, the MOPSO is applied, Table 5, where, the results obtained by both methods are closes to each other.

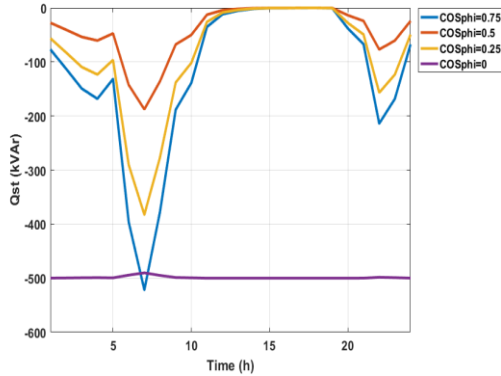


Fig 24: Reactive power variations due to the storage in bus 16 in the test network B for different power factors

Table 5: Comparison of simulation results by two MOPSO and NSGAI for the test network B

$\cos \varphi_{\text{lim}} = 1$	$\cos \varphi_{\text{lim}} = 0.75$	$\cos \varphi_{\text{lim}} = 0$	BESS	Algorithm	
7	7	7	-	NSGAI	D-STATCOM Location
7	7	7	-	MOPSO	
2500	2500	2500	-	NSGAI	D-STATCOM Capacity (kVAR)
2560	2560	2560	-	MOPSO	
1964	1944	1876	2438	NSGAI	Losses (kW)
1958	1938	1869	2438	MOPSO	

Conclusion

A hybrid method is proposed based on sensitivity analysis, multi-objective intelligent algorithm, fuzzy control and backward/forward method as to determine the location and optimal capacities of BESS and D-FACTS devices are applied to achieve the lowest network losses, increasing voltage static stability. In this process, first, by running the sensitivity analysis, the optimal location of the BESS installation is determined and next, by applying this hybrid method and the fuzzy controller for energy management, the optimal capacity of equipment is determined. In the studied networks, two distributed photovoltaic and wind generation units are of concern. The results of the simulations indicate that this proposed method will reduce network losses and improve voltage profile of the network buses. To apply the BESS inverter capability for reactive power generation, the BESS behavior is measured at different power factors and the effectiveness of BESS power factor on the indices of this study is assessed.

References

- [1] P. Qaderi-Baban, M.B. Menhaj, M. Dosaranian-Moghadam, And A. Fakharian, "Intelligent multi-agent system for DC microgrid energy coordination control", Bulletin of the Polish Academy of Sciences: Technical Sciences, DOI: 10.24425/bpasts.2019.130183.
- [2] M. Michalczuk, L.M. Grzesiak, And B. Ufnalski "Hybridization of the lithium energy storage for an urban electric vehicle", Bulletin of

the Polish Academy of Sciences: Technical Sciences, DOI: 10.2478/bpasts-2013-0030

- [3] Ali Ehsan, Qiang Yang, "Optimal integration and planning of renewable distributed generation in the power distribution networks: A review of analytical techniques", Applied Energy, DOI: 10.1016/j.apenergy.2017.10.106.
- [4] Keyan Liu, Wanxing Sheng, Yuan Liu, Xiaoli Meng, "Optimal sitting and sizing of DGs in distribution system considering time sequence characteristics of loads and DGs", European Journal of Engineering and Technology Research, Vol 4 No 10, 2019.
- [5] A. Lashkrara, H.B.Tolabi, "Nonlinear Modeling and Controller Design of DSTATCOM in a Microgrid Based on Combination of Fuzzy Set and Bees Algorithm", Computational Intelligence in Electrical Engineering. Vol. 7, No. 4, pp. 57-66, 2017.
- [6] M.Hosseini, H.A.Shayanfar, M.Futohi-Firozabad, "Modeling of Series and Shunt Distribution FACTS Devices in Distribution Systems Load Flow", Journal of Electrical Systems. Vol. 4, No. 4, pp. 1-12, 2008.
- [7] N.Ghaffarzadeh, A.Salimi, "A New Control Method of Photovoltaic-Battery Hybrid System Connected to the Electrical Network by Using Model Predictive Controller", Computational Intelligence in Electrical Engineering. Vol. 7, No. 2, pp. 29-40, 2016.
- [8] S.Jazebi, S.H. Hosseini, B. Vahidi, "DSTATCOM Allocation in Distribution Networks Considering Reconfiguration Using Differential Evolution Algorithm", Energy Conversion and Management. Vol. 52, No. 7, pp. 2777-2783, 2011.
- [9] S.A.Taher, S.A.Afsari, "Optimal Location and Sizing of DSTATCOM in Distribution Systems by Immune Algorithm", International Journal of Electrical Power and Energy Systems. Vol. 60, pp. 34-44, 2014.

- [10] G.Balakrishna, C.S.Babu, "Multi objective Distributed Generators and DSTATCOM Siting and Sizing by Modified Particle Swarm Optimization", International Advanced Research Journal in Science Engineering and Technolog. Vol. 2, No. 12, pp. 154–159, 2015.
- [11] J.Sanami, S.Gangull, A.K. Panda, "Allocation of DSTATCOM and DG in distribution systems to reduce power loss using ESM algorithm, Power Electronics", IEEE International Conference on Intelligent Control and Energy Systems (ICPEICES). pp. 1–5, 2017.
- [12] K.R. Devabalaji, K.Ravi, "Optimal size and siting of multiple DG and DSTATCOM in Radial Distribution System Using Bacterial Foraging Optimization Algorithm", Ain Shams Engineering Journal. Vol. 7, No. 3, pp. 959–971, 2016.
- [13] T.Yuvaraj, K.Ravi, K.R.Devabalaji, "Optimal Allocation of DG and DSTATCOM in Radial Distribution System Using Cuckoo Search Optimization Algorithm", Modeling and Simulation in Engineering. Vol. 2017, pp. 268–279, 2017.
- [14] F.Iqbal, M.Tauseef Khan, A.S. Siddiqui, "Optimal Placement of DG and DSTATCOM for Loss Reduction and Voltage Profile Improvement", Alexandria Engineering Journal. pp. 1–11, 2017.
- [15] K.Ravi, R.K.Devabalaji, "DSTATCOM Allocation in Distribution Networks Considering Load Variations Using Bat Algorithm", Ain Shams Engineering Journal. Vol. 8, pp. 391–403, 2017.
- [16] H.B.Tolabi, H.M.Ali, M.Rizwan, "Simultaneous Reconfiguration Optimal Placement of DSTATCOM, and Photovoltaic Array in a Distribution System Based on Fuzzy-ACO Approach", IEEE Transaction on Sustainable Energy Journal. Vol. 6, No. 1, pp. 210–218, 2015.
- [17] M.Mohammadi, M.Abasi, A. M. Rozbahani, "Fuzzy-GA Based Algorithm for Optimal Placement and Sizing of Distribution Static Compensator (DSTATCOM) for Loss Reduction of Distribution Network Considering Reconfiguration", Journal of Central South University. Vol. 24, No. 2, pp. 245–258, 2017.
- [18] P. Lazzeronia, M. Repettob, "Optimal planning of battery systems for power losses reduction in distribution grids", Electric Power Systems Research, 2019.
- [19] Dario Garozzo, Giuseppe Marco Tina, "Evaluation of the Effective Active Power Reserve for Fast Frequency Response of PV with BESS Inverters Considering Reactive Power Control", Energies, 2020.
- [20] T. Ahmadzadeh, E. Babaei, M. Sabahi, T. Abedinzadeh, "An Improved Transformerless Grid-Connected PV System with Related Control Strategy to Reduce Leakage Current, Extract Maximum Power Point and Control Power", Iranian Journal of Electrical and Electronic Engineering 04 (2020) 513–523.

APPENDIX

Table 6: Transformer information of the test network A

S_n [MVA]	Z_n [p.u.]	V_2 [kV]	V_1 [kV]	Node to	Node from
25	0.001+j0.12	20	110	1	0
25	0.001+j0.12	20	110	12	0

Table 7: Line information of the test network A

Node from	Node to	Length[km]	$R(\Omega)$	$X(\Omega)$	Installation
1	2	2.82	0.7529	0.5732	Underground
2	3	4.42	0.1801	0.8984	Underground
3	4	0.61	0.1629	0.1240	Underground
4	5	0.56	0.1495	0.1138	Underground
5	6	1.54	0.4112	0.3130	Underground
6	7	0.24	0.0641	0.0488	Underground
7	8	1.67	0.4459	0.3395	Underground
8	9	0.32	0.0854	0.0650	Underground
9	10	0.77	0.2056	0.1565	Underground
10	11	0.33	0.0881	0.0671	Underground
11	4	0.49	0.1308	0.0996	Underground
3	8	1.30	0.3471	0.2642	Underground
12	13	4.89	2.2240	1.7914	Overhead
13	14	2.99	1.3599	1.0953	Overhead
14	8	2.0	0.9096	0.7327	Overhead

Table 8: Load information of the test network A

BUS	(kVA) Peak apparent power[kVA]		Power factor(ind.)	
	Residential	Industrial	Residential	Industrial
1	15300	5100	0.98	0.95
2	-	-	-	-

3	285	265	0.97	0.85
4	445	-	0.97	-
5	750	-	0.97	-
6	565	-	0.97	-
7	-	90	-	0.85
8	605	-	0.97	-
9	-	675	-	0.85
10	490	80	0.97	0.85
11	340	-	0.97	-
12	15300	5280	0.98	0.85
13	-	40	-	0.85
14	215	390	0.97	0.85

Table 9: Line information of the test network B

Node from	Node to	$R(\Omega)$	$X(\Omega)$
1	2	0.00312	0.06753
2	3	0.00431	0.01204
3	4	0.00601	0.01677
4	5	0.00316	0.00882
5	6	0.00896	0.02502
6	7	0.00295	0.00824
7	8	0.01720	0.02120
8	9	0.04070	0.03053
3	10	0.01706	0.02209
2	11	0.02910	0.03768
11	12	0.02222	0.02877
12	13	0.04803	0.06218
12	14	0.03985	0.05160
14	15	0.02910	0.03768
14	16	0.03727	0.04593
16	17	0.02208	0.02720

Table 10: Load information of the test network B

Busburb	Real power[kW]	Reactive power[kVAr]	Power factor(ind.)
1	-	-	-
2	-	-	-
3	200	120	0.86
4	400	250	0.85
5	1500	930	0.85
6	3000	2260	0.80
7	800	500	0.85
8	200	120	0.86
9	1000	620	0.85
10	500	310	0.85
11	1000	620	0.85
12	300	190	0.84
13	200	120	0.86
14	800	500	0.85
15	500	310	0.85
16	1000	620	0.85
17	200	120	0.86